

Ab initio calculation of the phonon-induced contribution to the electron-state linewidth on the Mg(0001) surface versus bulk Mg

A. Leonardo,^{1,2} I. Yu. Sklyadneva,^{1,3} V. M. Silkin,² P. M. Echenique,^{1,2} and E. V. Chulkov^{1,2}

¹*Departamento de Física de Materiales and Centro Mixto CSIC-UPV/EHU, Facultad de Ciencias Químicas, UPV/EHU, Apartado 1072, 20080 San Sebastián/Donostia, Basque Country, Spain*

²*Donostia International Physics Center (DIPC), 20018 San Sebastián/Donostia, Basque Country, Spain*

³*Institute of Strength Physics and Materials Science, Prospekt Akademicheskii 2/1, 634021 Tomsk, Russia*

(Received 17 May 2007; published 5 July 2007)

We report a detailed *ab initio* study of the electron-phonon (e-ph) interaction contribution to the linewidth $\Gamma_{e-ph}(\epsilon_{\mathbf{k},i})$ of electron and hole states for bulk magnesium and the Mg(0001) surface. The calculations are based on density functional theory and linear response approach. For bulk Mg, we find a large contribution of optical phonons to the Eliashberg spectral function and to $\Gamma_{e-ph}(\epsilon_{\mathbf{k},i})$. The e-ph coupling parameter λ at the Fermi level (mass enhancement parameter) has been found to be $\lambda=0.30$. In the case of the surface, we have focused on the study of the $\bar{\Gamma}$ and \bar{M} surface states for which we find $\lambda=0.28$ and $\lambda=0.38$, respectively. We show an important role of the Rayleigh vibrational mode in the e-ph coupling in the $\bar{\Gamma}$ surface state. These results are in a very good agreement with tunneling spectroscopic data and recent photoemission measurements of λ .

DOI: [10.1103/PhysRevB.76.035404](https://doi.org/10.1103/PhysRevB.76.035404)

PACS number(s): 79.20.Uv, 71.45.Gm, 71.15.Mb, 71.15.Dx

I. INTRODUCTION

For the past decade, enormous progress in the study of electron and hole dynamics in bulk metals and at metal surfaces has been achieved both theoretically and experimentally.¹⁻¹⁷ Interest in this study is motivated by an essential role which electron excitations play in many chemical and physical phenomena. They are of paramount importance for energy transfer in photochemical reactions,¹⁸ for excitation mediated desorption and oxidation of molecules at surfaces¹⁹ as well as for electron localization at interfaces.²⁰ Electron excitations are essential for catalytical reactions as well as for charge and spin transport in bulk metals, across interfaces, and at surfaces.²¹⁻²³ The key quantity for these processes is the lifetime τ of the excited electron which sets the duration of the excitation and in combination with the velocity determines the mean free path of the excited particle. The lifetime, or the lifetime broadening Γ ($\Gamma_{tot}=\Gamma_{e-e}+\Gamma_{e-ph}=\hbar/\tau$) in paramagnetic metals, is determined by inelastic electron-electron (e-e) scattering and electron-phonon (e-ph) interaction. In general, the experimentally measured broadening is also influenced by elastic electron-defect scattering. However, this type of scattering can be avoided in scanning tunneling spectroscopy measurements^{8,12,15} and in time-resolved two-photon-photoemission experiments.^{1,11,12} It can also be strongly reduced in photoemission spectroscopy studies.^{9,12}

The e-e contribution Γ_{e-e} to the lifetime broadening has been studied theoretically within a *GW* approximation for bulk,^{7,17} surface,^{8,10,12} image potential,^{5,10,12} quantum well,²⁴ and adsorbate²⁵ excited electron (hole) states. It was shown that for excitation energies in the range from 1 to 5 eV and at low temperatures, the e-e contribution is, in general, significantly larger than the e-ph one.^{12,17,26} For energies close to the Fermi energy, Γ_{e-ph} can be comparable with Γ_{e-e} ,^{12,17,24,27,28} and at room temperature, it can be much larger than Γ_{e-e} .^{17,26}

Up to now, the majority of evaluations of Γ_{e-ph} (Refs. 8, 24, and 29-35) have been done by assuming a constant e-ph

coupling matrix element $g(\mathbf{k}_i, \mathbf{k}_f, \mathbf{q}, \omega)$ and using a Debye model for the phonon spectrum of a system.³⁶ In this approach, the Eliashberg spectral function $\alpha^2F(\omega)$ and the e-ph coupling strength parameter λ are determined by density of phonon states only and do not depend on an electron state. Recently, a more complex model for calculating e-ph interaction in surface states has been proposed.^{28,37,38} The model combines three independent approximations to evaluate the e-ph coupling matrix elements: (1) one-electron wave functions and energies are calculated with one-dimensional potential,³⁹ (2) phonon frequencies and polarizations are obtained from one-parameter force-constant model,⁴⁰ and (3) a gradient of one-electron potential is represented by using the Ashcroft pseudopotential⁴¹ screened within Thomas-Fermi approximation. However, this model can only be applied to *s-p_z* surface states on simple and noble metal surfaces. An advantage of *ab initio* calculations is that all the three ingredients of the e-ph coupling matrix elements are precisely evaluated on the same footing irrespectively to the surface state symmetry. Fully *ab initio* calculations of e-ph interaction for excited electrons and holes have been done recently for bulk Be (Ref. 26) and Pd (Ref. 42) as well as for the $\bar{\Gamma}$ surface state on Be(0001) (Ref. 43) and Al(100) (Ref. 44). It was shown that the e-ph coupling in the $\bar{\Gamma}$ surface state on Be(0001) is much stronger than that in bulk Be (Ref. 43) while on Al(100), the λ value is only 20% larger than in bulk Al.⁴⁴ It was also demonstrated a very important role of the Rayleigh vibrational mode contribution to the Eliashberg spectral function and λ for these surface states of the *s-p_z* symmetry.^{43,44}

In this work, we analyze the dependence of the e-ph interaction with respect to the symmetry of the surface state, using the Mg(0001) surface as an example. Magnesium, in contrast to transition metals, is not catalytically active and is not used for energy or spin transport. However, *ab initio* calculations of e-ph interaction on simple metal surfaces are significantly less time consuming than those on transition metal surfaces, and some key features of e-ph interaction can

be understood from the exploration of simple metal surfaces. The Mg(0001) surface electronic structure has been studied in detail both experimentally, by using photoemission spectroscopy,⁴⁵⁻⁴⁷ and theoretically, by using *ab initio* calculations.⁴⁸ Two clear surface states of different symmetries have been found: one at the $\bar{\Gamma}$ point (s - p_z symmetry) and the other at the \bar{M} point ($p_{x,y}$ symmetry). We present *ab initio* calculation results for the Eliashberg spectral function $\alpha^2F(\omega)$, e-ph coupling parameter λ , and phonon-induced contribution Γ_{e-ph} to the lifetime broadening of the $\bar{\Gamma}$ and \bar{M} surface states on Mg(0001) as well as of electron states in bulk Mg. We demonstrate strong momentum dependence of $\alpha^2F(\omega)$, λ , and Γ_{e-ph} for both bulk Mg and Mg(0001). We find that the e-ph coupling in the \bar{M} surface state is much stronger than that in the $\bar{\Gamma}$ surface state. This is accounted for by the strong interaction with bulk phonon modes. In contrast to the $\bar{\Gamma}$ surface state on Mg(0001) [as well as on Be(0001) (Ref. 43) and Al(100) (Ref. 44)], the e-ph coupling of the \bar{M} surface state with the Rayleigh mode vibrations is relatively small. Excellent agreement with available experimental λ is obtained for both bulk Mg and the Mg(0001) surface. For the discussion of the role of different contributions to the lifetime broadening, we also present the *GW* calculations of Γ_{e-e} for selected electron states in these systems.

The paper is organized as follows. In Sec. II, a short outline of the calculation method is given. In Sec. III, we present and discuss the calculation results and in Sec. IV, the conclusions are drawn.

II. THEORY

Phonon-induced contribution to electron linewidths (lifetimes) due to the electron-phonon interaction may be computed from the imaginary part of the electron-phonon self-energy. Equation (1) shows the linewidth of an initial electronic state ($\epsilon_{\mathbf{k},i}$) scattered by a phonon of a frequency ω and to a final electron state ($\epsilon_{\mathbf{k},f}$):³⁶

$$\Gamma_{e-ph}(\epsilon_{\mathbf{k},i}) = \tau_{e-ph}^{-1}(\epsilon_{\mathbf{k},i}) = 2\pi \int_0^{\omega_m} \alpha^2 F_{\mathbf{k},i}(\omega) [1 - f(\epsilon_{\mathbf{k},i} - \omega) + f(\epsilon_{\mathbf{k},i} + \omega) + 2n(\omega)] d\omega. \quad (1)$$

Here, $f(\epsilon_{\mathbf{k},i} \pm \omega)$ and $n(\omega)$ are the Fermi and Bose distributions, respectively, which introduce a temperature dependence of the lifetime (linewidth) and ω_m is the maximum phonon frequency. $\alpha^2 F_{\mathbf{k},i}(\omega)$ is the electron-state-dependent Eliashberg spectral function which *measures* the effectiveness of phonons of energy $\hbar\omega$ to scatter an electron (hole) in a selected initial state $\epsilon_{\mathbf{k},i}$:

$$\alpha^2 F_{\mathbf{k},i}(\omega) = \sum_{\mathbf{q},\nu} \delta(\omega - \omega_{\mathbf{q},\nu}) |g(\mathbf{k}_i, \mathbf{k}_f, \mathbf{q}, \nu)|^2 \delta(\epsilon_{\mathbf{k},f} - \epsilon_{\mathbf{k},i}). \quad (2)$$

The sum in Eq. (2) is performed over final electron states \mathbf{k}_f and all possible phonon modes ν with momentum \mathbf{q} . Note

that Eq. (2) is obtained within quasielastic scattering approximation where $\delta(\epsilon_{\mathbf{k},i} - \epsilon_{\mathbf{k},f} \pm \omega_{\mathbf{q},\nu}) \approx \delta(\epsilon_{\mathbf{k},i} - \epsilon_{\mathbf{k},f})$. $g(\mathbf{k}_i, \mathbf{k}_f, \mathbf{q}, \nu)$ is the electron-phonon coupling matrix element

$$g(\mathbf{k}_i, \mathbf{k}_f, \mathbf{q}, \nu) = \sqrt{\frac{\hbar}{2M\omega_{\mathbf{q},\nu}}} \langle \psi_{\mathbf{k}+\mathbf{q},f} | \hat{\epsilon}_{\mathbf{q},\nu} \cdot \nabla_{\mathbf{R}} V_{\mathbf{q}}^{sc} | \psi_{\mathbf{k},i} \rangle, \quad (3)$$

where M is the atom mass, $\hat{\epsilon}_{\mathbf{q},\nu}$ are the phonon polarization vectors, and $\nabla_{\mathbf{R}} V_{\mathbf{q}}^{sc}$ is the gradient of the screened one-electron potential with respect to atom displacements $\hat{\epsilon}_{\mathbf{q},\nu}$ from their equilibrium positions \mathbf{R} .

The electron-state-dependent strength of electron-phonon coupling is measured by the dimensionless parameter λ defined as

$$\lambda(\epsilon_{\mathbf{k},i}) = 2 \int_0^{\omega_m} \frac{\alpha^2 F(\epsilon_{\mathbf{k},i}; \omega)}{\omega} d\omega. \quad (4)$$

When initial and final electronic states remain on the Fermi surface ($\epsilon_{\mathbf{k},i} = \epsilon_{\mathbf{k},f} = E_F$), a function averaged over the Fermi surface can be defined by considering the sum over all the possible initial electron states:⁴⁹

$$\alpha^2 F(\omega) = \frac{1}{N(E_F)} \sum_{\mathbf{q},\nu} \delta(\omega - \omega_{\mathbf{q},\nu}) \sum_{\mathbf{k},i,f} |g(\mathbf{k}_i, \mathbf{k}_f, \mathbf{q}, \nu)|^2 \times \delta(\epsilon_{\mathbf{k},i} - E_F) \delta(\epsilon_{\mathbf{k},f} - E_F). \quad (5)$$

Here, $N(E_F)$ is the electron density of states per atom and per spin at the Fermi level E_F . With this $\alpha^2 F(\omega)$ and following Eq. (4), one can obtain the e-ph coupling parameter λ for electronic states at E_F , also known as the mass enhancement parameter.

Electronic structure of bulk Mg and Mg(0001) has been calculated within *ab initio* pseudopotential local-density-approximation formalism with a plane wave basis code.⁵⁰ Norm-conserving pseudopotential with a nonlinear core correction was generated by using the method of von Barth and Car direct fit.⁵⁰ The local exchange-correlation functional was taken in the Perdew-Zunger form. To obtain the phonon spectra, as well as the matrix elements of e-ph interaction, we chose the density functional perturbation theory^{51,52} and adopted the usual adiabatic approximation. For both bulk and surface calculations, the Hermite-Gauss smearing technique⁵³ with a smearing width of $\sigma = 30$ mRy was employed.

Electron-electron contribution Γ_{e-e} to the lifetime broadening of electron and hole states for bulk Mg is obtained in the framework of many-body theory on the energy-shell approximation in terms of the imaginary part of the complex nonlocal self-energy operator.¹² This quantity is evaluated in the *GW* approximation. Further details of the calculation can be found in Ref. 54. Specific details of the present calculation are (1) the inclusion of 40 reciprocal vectors in the dielectric matrix expansion, (2) the use of $24 \times 24 \times 16$ mesh for all k -space integrations, and (3) the inclusion of all occupied and unoccupied one-electron energy bands up to 50 eV above the Fermi level, in the evaluation of density response matrix.

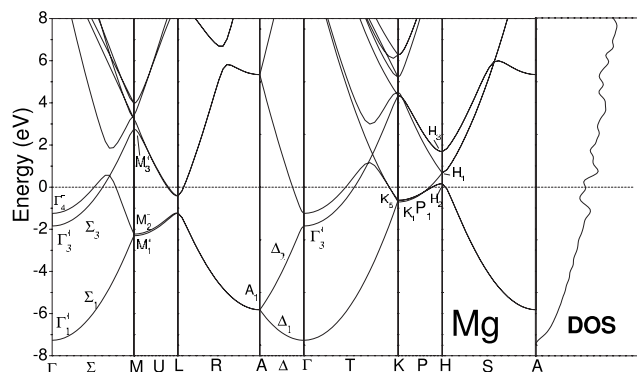


FIG. 1. Electron energy bands for bulk Mg. The right panel shows density of electron states.

III. RESULTS AND DISCUSSION

A. Bulk magnesium

Bulk magnesium has a hcp structure with experimentally measured⁵⁵ lattice parameters $a=3.21$ Å and $c/a=1.623$. In order to obtain the correct vibrational modes, it is crucial for the calculation to have the correct equilibrium lattice parameters which were found to be in our case $a=3.13$ Å and $c/a=1.623$. This difference between experimental and evaluated lattice parameters is a typical local-density-approximation (LDA) effect and is in good agreement with other theoretical works^{56,57} based on LDA. As already mentioned, the complete electron and phonon spectra are needed for further calculations. These spectra computed with equilibrium lattice parameters are shown in Figs. 1 and 2, respectively. Electron density of states in the right panel of Fig. 1 shows a nearly free-electron-like behavior as it is expected for Mg. In the case of phonons, except for the fact that optical branches are slightly overestimated, the general agreement with neutron scattering data⁵⁸ is good.

Our theoretical evaluation of the mass enhancement parameter has been performed integrating over 84 phonon wave vectors \mathbf{q} inside the irreducible Brillouin zone (1000 in the whole zone) and 610 electronic wave vectors \mathbf{k} . The resulting Eliashberg function, $\alpha^2F(\omega)$, averaged over momenta at the Fermi level is shown in Fig. 3 together with experimental data,⁵⁹ the calculated phonon density of states

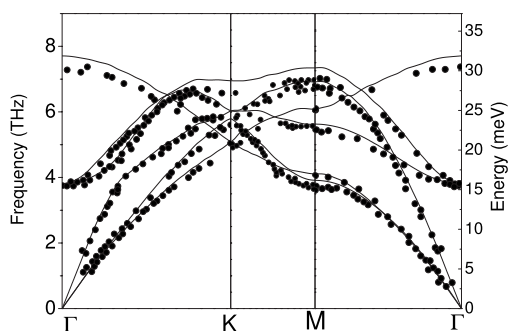


FIG. 2. Calculated phonon dispersion curves of bulk Mg along the high-symmetry directions. The solid circles show the experimentally measured frequencies (Ref. 58).

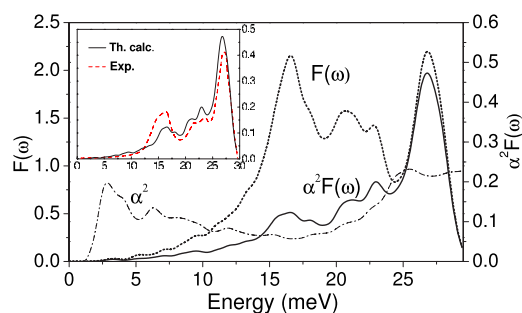


FIG. 3. (Color online) Phonon density of states $F(\omega)$ (dotted line) and electron-phonon spectral function $\alpha^2F(\omega)$ (solid line) calculated at E_F are depicted with different scales. The frequency-dependent coupling function α^2 [defined as the ratio $\alpha^2F(\omega)/F(\omega)$] is shown by dash-dotted line. The inset panel compares calculated (solid line) and experimental (Ref. 59) (dashed line) $\alpha^2F(\omega)$.

$F(\omega)$, and the coupling function α^2 . Magnesium due to its relatively low electron-phonon coupling is believed to become superconductor at temperatures below 0.5 mK,^{60,61} and it is the reason why it is inaccessible to conventional tunneling spectroscopy. In order to obtain the Eliashberg spectral function experimentally, a strong coupling superconductor is approximated to induce superconductivity in Mg. Burnell and Wolf⁵⁹ have performed such experiments and their results are shown in the inset of Fig. 3. The overall agreement in the shape of the Eliashberg function and in the position of the peaks is remarkable. The greatest difference between both curves occurs at 16 meV where the matrix elements lower strongly the existing maxima of the phonon density of states. From the figure, it is clearly seen that high frequency optical phonon modes mostly contribute to the scattering processes of electrons while lower frequency phonons are suppressed. This is an expected behavior for the hcp simple metals that has previously been found by Sklyadneva *et al.*²⁶ for beryllium.

In Table I, we show the calculated mass enhancement parameter λ together with other experimental⁵⁹ and theoretical^{49,62,63} values. One can see that our λ is in excellent agreement with the measured mass enhancement parameter value and with other theoretical data.

More information on the e-ph interaction can be obtained from the momentum-dependent study of the Eliashberg spectral function and λ in different occupied and unoccupied electron states. In Fig. 4, we show the calculated $\alpha^2F_{\mathbf{k},i}(\omega)$ and $\lambda(\epsilon_{\mathbf{k},i})$ for several electron states at symmetry points

TABLE I. The calculated and measured mass enhancement parameter λ in bulk Mg.

λ	References
0.35	62 (Calc.)
0.31	63 (Calc.)
0.33 ± 0.03	49 (Calc.)
0.29 ± 0.03	59 (Expt.)
0.30	Present work

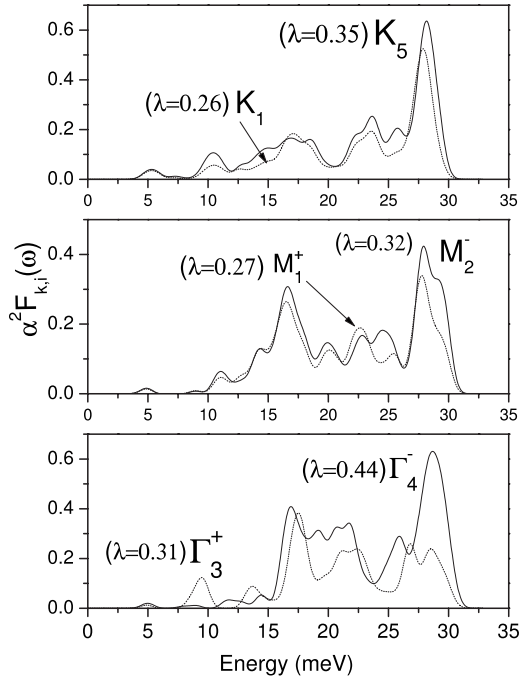


FIG. 4. Electron-phonon spectral function $\alpha^2 F_{\mathbf{k},i}(\omega)$ in bulk Mg for several electron states at the K , M , and Γ symmetry points.

K , M , and Γ . Even though the behavior of $\alpha^2 F_{\mathbf{k},i}(\omega)$ and the $\lambda(\epsilon_{\mathbf{k},i})$ values is, in general, much unpredictable, there exist some common features. The high frequency phonon scattering predominance is clear for all selected initial electronic states, and the optical phonon peak at around 27 meV is still the strongest coupling mode. Another feature is the increasing value of λ as the electron state approaches the Fermi level. This is clear at the Γ point, where a significant difference exists between the values at the Γ_3^+ ($\lambda=0.31$) point and at Γ_4^- ($\lambda=0.44$) closer to the Fermi level.

Up to now, we have discussed in detail linewidths and Eliashberg functions of electron states due to the e-ph interaction. In Table II, we present the calculation results of the contribution to the linewidth of the e-e interaction Γ_{e-e} at symmetry points performed within *GW* approximation. In general, the Γ_{e-e} contribution to the total linewidth is larger than the corresponding Γ_{e-ph} , especially at low temperatures.

TABLE II. Decay rates Γ_{e-e} and Γ_{e-ph} of selected electron (hole) states at symmetry points of the Brillouin zone (in meV). The state energies E are relative to E_F .

State	E (eV)	Γ_{e-e}	Γ_{e-ph} $T=0$ K	Γ_{e-ph} $T=300$ K
Γ_3^+	-1.74	77	19	53
Γ_4^-	-1.26	57	30	77
K_1	-0.68	16	17	47
K_5	-0.60	10	22	63
M_1^+	-2.30	150	17	48
M_2^-	-2.22	136	21	55
M_3^+	+2.75	182	27	76

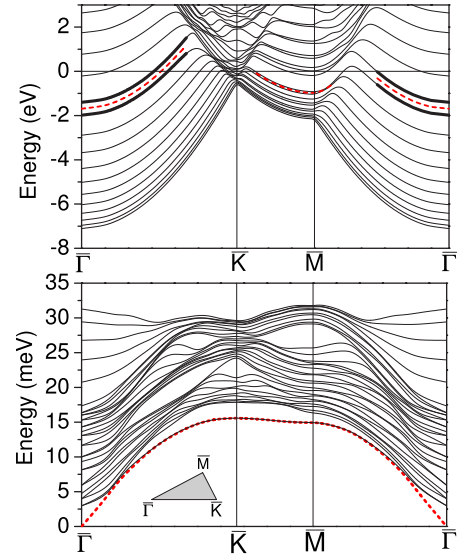


FIG. 5. (Color online) Top panel shows the electronic band structure of a fully relaxed 11 layer Mg(0001) slab; $\bar{\Gamma}$ and \bar{M} surface states are indicated by a dashed line which correspond to the average of the thick solid lines representing surface state dispersions obtained in the slab calculation. Horizontal line indicates the Fermi energy. Bottom panel shows the phonon dispersions, where dotted line corresponds to the Rayleigh mode.

However, with the increase of temperature, Γ_{e-ph} increases linearly with T (for relatively high T) while Γ_{e-e} remains constant. Values of Γ_{e-e} shown in the table follow this trend when compared to Γ_{e-ph} . Exceptions are electron states K_1 and K_5 for which even at $T=0$, both Γ_{e-e} and Γ_{e-ph} are comparable.

B. Mg(0001) surface

A periodically repeated slab geometry with Mg(0001) slabs of 11 atomic layers separated by a vacuum region of 18 Å was used to study the surface electronic structure, phonon spectrum, and e-ph interaction. In order to obtain a good structural and dynamical description of the system, an energy minimization was performed allowing the variation of the interlayer distances. Since the surface is unreconstructed, the atomic positions inside the plane maintain the hexagonal symmetry of the bulk and the lattice parameter a is kept to be 3.13 Å. Forces between atoms in the perpendicular direction were relaxed and checked to be smaller than 10^{-4} Ry/a.u.. The interlayer relaxation calculations give expansion of the first and the second interlayer spacing relative to the bulk of $\Delta d_{12} = +1.6\%$ and $\Delta d_{23} = +0.3\%$, respectively. These results are close to experimental data obtained by Sprunger *et al.*,⁶⁵ $\Delta d_{12} = (+1.9 \pm 0.3)\%$ and $\Delta d_{23} = (+0.8 \pm 0.4)\%$. Other theoretical work by Wright *et al.*⁶⁶ reports values of $\Delta d_{12} = +1.5\%$ and $\Delta d_{23} = +0.5\%$.

In Fig. 5, we show the calculated electron and phonon spectra of the surface. In the top panel corresponding to electronic states, dashed lines represent surface states at $\bar{\Gamma}$ and \bar{M} with energy values relative to the Fermi level of 1.69 and 0.98 eV. Recently, angle-resolved photoemission experi-

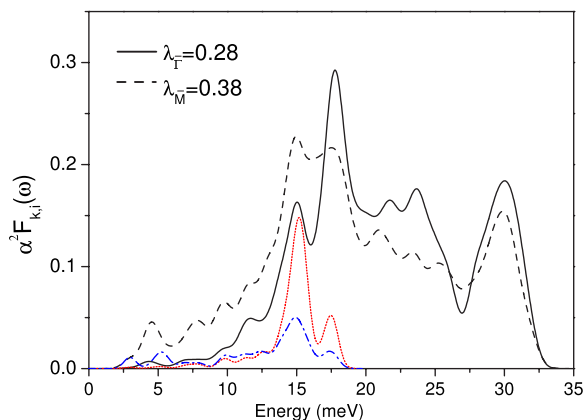


FIG. 6. (Color online) The solid line represents the Eliashberg function of the surface state at the $\bar{\Gamma}$ point while the dashed line is for the surface state at \bar{M} . The dotted (dash-dotted) line represents the contribution of the Rayleigh mode to the Eliashberg function of the surface state at the $\bar{\Gamma}$ (\bar{M}) point.

ments (ARPES) by Schiller *et al.*⁴⁷ find surface states at -1.63 ± 0.06 and -0.95 ± 0.05 eV, respectively. In the bottom panel where the phonon dispersion for Mg(0001) is presented, the surface Rayleigh mode is shown by a dotted line. The vibration amplitude of this mode is mainly perpendicular to the surface and decays exponentially into the bulk. The resulting phonon energies obtained are of 15.6 and 14.9 meV at the \bar{K} and \bar{M} points, respectively. The other *ab initio* calculation has reported 14.9 and 14.2 meV,⁵⁷ and experimental measurements performed with momentum-resolved inelastic electron scattering give values of 14.2 and 13.5 meV.⁵⁷

In Fig. 6, we show the calculated Eliashberg spectral function of surface states at the $\bar{\Gamma}$ (solid line) and \bar{M} (dashed line) points. These two curves include coupling to all bulk and surface phonon modes. Separately, we also show the Rayleigh mode contribution to $\alpha^2 F_{\mathbf{k}_i}(\omega)$ for the $\bar{\Gamma}$ (dotted line) and \bar{M} (dash-dotted line) surface states. As follows from the figure, a pronounced peak for the $\bar{\Gamma}$ state corresponding to the coupling to the Rayleigh mode arises at around 15 meV. This is an expected feature since the $\bar{\Gamma}$ surface state has $s-p_z$ symmetry,⁴⁸ i.e., the probability density amplitude of this state is distributed in the perpendicular direction, parallel to the Rayleigh mode polarization and to the gradient of the one-electron potential. The large overlap between the surface electron wave function and the dominant direction of the phonon mode and of the gradient turns into a fairly big value of the matrix element. The \bar{M} surface state is of the p_x, p_y symmetry, i.e., the probability density amplitude of the state is distributed in the interstitial regions of several surface atomic layers.⁴⁸ Hence, the overlap with the Rayleigh mode and with the one-electron gradient should not be large so the corresponding contribution should be small. These qualitative arguments are corroborated by the dash-dotted line in Fig. 6. Nevertheless, the spectral function of the \bar{M} surface state is very big in the energy interval between 14 and 18 meV. This can be accounted for by the coupling to

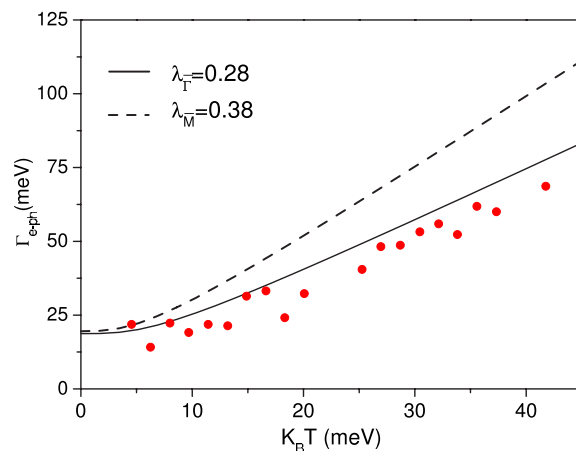


FIG. 7. (Color online) Temperature dependence of the surface state linewidths at the $\bar{\Gamma}$ and \bar{M} points. Red dots represent experimental data extracted from Ref. 35; they were plotted by subtracting an offset that corresponds to $\Gamma_{e-e} + \Gamma_{e-def}$.

bulk phonon modes: precisely, in this energy interval, the bulk phonon density of states of Mg (Fig. 3) shows a very strong peak that favors the spectral function at these energies.

Valuable information can be obtained from the temperature dependence of the linewidth of a quantum state of interest. As already mentioned, the temperature dependence of the linewidth comes from the Bose and Fermi distribution functions. In order to plot Γ_{e-ph} versus T numerically, calculated Eliashberg spectra $\alpha^2 F(\omega)$ are inserted in Eq. (1). The resulting Γ_{e-ph} presented in Fig. 7 shows the correct linear behavior³⁶ at high temperatures ($k_B T \gg \omega_m$) $\Gamma_{ep}(\mathbf{k}_i, E) = 2\pi\lambda(\mathbf{k}_i)k_B T$. ARPES experiments determine λ by plotting the graph from the corresponding experimental data. Supposing that the temperature dependence of the electronic lifetime comes only from the e-ph interaction, linewidths of selected quantum states can be measured for different temperatures and λ can be deduced from the slope of the graph. This has been done by Kim *et al.*³⁵ for the surface state at the $\bar{\Gamma}$ point using a three-dimensional Debye model to obtain the Eliashberg function [$\alpha^2 F_{\mathbf{k}_i}(\omega) = \lambda \omega^2 / \omega_D^2$]. Dots in Fig. 7 represent experimental data extracted from Ref. 35 where a value of $\lambda = 0.27(2)$ has been reported for the $\bar{\Gamma}$ surface state. This value is in excellent agreement with our calculated result, $\lambda_{\bar{\Gamma}} = 0.28$.

In Table III, we show the e-e and e-ph contributions to the lifetime broadening for the $\bar{\Gamma}$ and \bar{M} surface states. The calculated e-e contribution has been taken from Ref. 67. For both surface states, this contribution is larger than the corresponding e-ph one. However, for the surface state at \bar{M} , as temperature increases, e-e and e-ph contributions become comparable and at room temperature Γ_{e-ph} is significantly larger than Γ_{e-e} . The total evaluated lifetime broadening $\Gamma_{calc}^{tot} = \Gamma_{e-e} + \Gamma_{e-ph} = 111$ meV may be compared to the experimental one of 133 meV reported by Kim *et al.*³⁵ which also includes the contribution from electron scattering on defects Γ_{e-def} . The difference between the theoretical value,

TABLE III. Linewidths (in meV) of surface states at $\bar{\Gamma}$ and \bar{M} . Γ_{calc}^{tot} is the sum of the e-e and e-ph contributions at $T=0$ K. The experimental value (Ref. 35) is obtained by extrapolating measured data to $T=0$ K.

	E (eV)	Γ_{e-ph} $T=0$ K	Γ_{e-ph} $T=300$ K	Γ_{e-e}	Γ_{calc}^{tot} $T=0$ K	$\Gamma_{expt.}$ $T=0$ K
$\bar{\Gamma}$	-1.69	19	52	92	111	133
\bar{M}	-0.98	20	65	32	52	

111 meV, and the measured one would give a rough estimation of the contribution to the linewidth due to the electron-defect interaction.

It is worthy to compare the *ab initio* evaluated e-ph contribution to the linewidth with that derived from the Debye model³⁶ mentioned in the Introduction. In the latter model, the phonon-induced lifetime broadening of electron states at $T=0$ K is reduced to $\Gamma_{e-ph}^D = 2\pi\lambda k_B \Theta_D / 3$, where k_B and Θ_D are the Boltzmann constant and Debye temperature, respectively. Using this equation with *ab initio* calculated $\lambda=0.28$, we find $\Gamma_{e-ph}^D = 20.2(16.1)$ meV for $\Theta_D=400(318)$ K taken from the Kittel⁶⁴ (Ashcroft and Mermin⁶⁸) book. The obtained Γ_{e-ph}^D are in fairly good agreement with *ab initio* $\Gamma_{e-ph}=19$ meV. Also, rather good accord with *ab initio* Γ_{e-ph} is found for the \bar{M} surface state: $\Gamma_{e-ph}^D = 27.4(21.8)$ meV is well compared to *ab initio* $\Gamma_{e-ph}=20$ meV. These results lend support to the practical use of the Debye model for fast estimations of the phonon-induced lifetime broadening of sur-

face electron states provided that the e-ph coupling parameter λ is known from *ab initio* calculations or photoemission measurements.

IV. SUMMARY AND CONCLUSIONS

We have presented a first-principles study of the electron-phonon contribution to the lifetime broadening of electron and hole states in bulk Mg and at the Mg(0001) surface. For bulk Mg, we have evaluated the mass enhancement parameter λ for selected electron states as well as averaged λ for the states at the Fermi surface. These values may differ significantly from one to another, but in general they increase as the electron state approaches the Fermi level. It has been shown that optical phonon modes mostly contribute to the electron-phonon coupling in electron states both at E_F and beyond. In the case of Mg(0001) surface, both surface states located at $\bar{\Gamma}$ and \bar{M} have been studied. The obtained results are in good agreement with available experimental data. We address the special relevance of the Rayleigh mode in the e-ph coupling in the surface state at $\bar{\Gamma}$ point. At the \bar{M} point, this coupling is mostly due to bulk phonon states.

ACKNOWLEDGMENTS

This work was partially supported by the University of the Basque Country, the Departamento de Educación del Gobierno Vasco, and MCyT (Grant No. FIS 2004-06490-C03-01).

- ¹U. Höfer, I. L. Shumay, Ch. Reuß, U. Thomann, W. Wallauer, and Th. Fauster, *Science* **277**, 1480 (1997).
²H. Petek and S. Ogawa, *Prog. Surf. Sci.* **56**, 239 (1997).
³M. Aeschlimann, M. Bauer, S. Pawlik, W. Weber, R. Burgermeister, D. Oberli, and H. C. Siegmann, *Phys. Rev. Lett.* **79**, 5158 (1997).
⁴E. Knoesel, A. Hotzel, and M. Wolf, *Phys. Rev. B* **57**, 12812 (1998).
⁵E. V. Chulkov, I. Sarría, V. M. Silkin, J. M. Pitarke, and P. M. Echenique, *Phys. Rev. Lett.* **80**, 4947 (1998); J. Osma, I. J. Sarría, E. V. Chulkov, J. M. Pitarke, and P. M. Echenique, *Phys. Rev. B* **59**, 10591 (1999).
⁶R. Matzdorf, *Surf. Sci. Rep.* **30**, 153 (1998).
⁷W.-D. Schöne, R. Keyling, M. Bandic, and W. Ekaradt, *Phys. Rev. B* **60**, 8616 (1999); I. Campillo, J. M. Pitarke, A. Rubio, E. Zarate, and P. M. Echenique, *Phys. Rev. Lett.* **83**, 2230 (1999); V. P. Zhukov, F. Aryasetiawan, E. V. Chulkov, I. G. de Gurtubay, and P. M. Echenique, *Phys. Rev. B* **64**, 195122 (2001); V. P. Zhukov, F. Aryasetiawan, E. V. Chulkov, and P. M. Echenique, *ibid.* **65**, 115116 (2002); F. Ladstädter, P. F. de Pablos, U. Hohenester, P. Puschnig, C. Ambrosch-Draxl, P. L. de Andrés, F. J. García-Vidal, and F. Flores, *ibid.* **68**, 085107 (2003).
⁸J. Kliewer, R. Berndt, E. V. Chulkov, V. M. Silkin, P. M. Echenique, and S. Crampin, *Science* **288**, 1399 (2000).
⁹F. Reinert, G. Nicolay, S. Schmidt, D. Ehm, and S. Hüfner, *Phys.*

- Rev. B* **63**, 115415 (2001).
¹⁰E. V. Chulkov, V. M. Silkin, and M. Machado, *Surf. Sci.* **693**, 482 (2001).
¹¹M. Weinelt, *J. Phys.: Condens. Matter* **14**, R1099 (2002).
¹²P. M. Echenique, R. Berndt, E. V. Chulkov, Th. Fauster, A. Goldman, and U. Höfer, *Surf. Sci. Rep.* **52**, 219 (2004).
¹³V. P. Zhukov, E. V. Chulkov, and P. M. Echenique, *Phys. Rev. Lett.* **93**, 096401 (2004).
¹⁴M. Sakaue, *J. Phys.: Condens. Matter* **17**, S245 (2005).
¹⁵J. Kröger, L. Limot, H. Jensen, R. Berndt, S. Crampin, and E. Pehlke, *Prog. Surf. Sci.* **80**, 26 (2005).
¹⁶J. Güdde and U. Höfer, *Prog. Surf. Sci.* **80**, 49 (2005).
¹⁷E. V. Chulkov, A. G. Borisov, J. P. Gauyacq, D. Sanchez-Portal, V. M. Silkin, V. P. Zhukov, and P. M. Echenique, *Chem. Rev. (Washington, D.C.)* **106**, 4160 (2006).
¹⁸*Laser Spectroscopy and Photochemistry on Metal Surfaces*, edited by H. L. Dai and W. Ho (World Scientific, Singapore, 1995).
¹⁹M. Bonn, S. Funk, C. Hess, D. N. Denzler, C. Stampfl, M. Scheffler, M. Wolf, and G. Ertl, *Science* **285**, 1042 (1999).
²⁰N. H. Ge, C. M. Wong, R. L. Lingle, Jr., J. D. McNeill, K. J. Gaffney, and C. B. Harris, *Science* **279**, 202 (1998).
²¹H. Nienhaus, *Surf. Sci. Rep.* **45**, 1 (2002).
²²R. Haight, *Surf. Sci. Rep.* **21**, 275 (1995).
²³I. Zutic, J. Fabian, and S. Das Sarma, *Rev. Mod. Phys.* **76**, 323

- (2004).
- ²⁴E. V. Chulkov, J. Kliewer, R. Berndt, V. M. Silkin, B. Hellsing, S. Crampin, and P. M. Echenique, *Phys. Rev. B* **68**, 195422 (2003).
- ²⁵A. G. Borisov, J. P. Gauyacq, A. K. Kazansky, E. V. Chulkov, V. M. Silkin, and P. M. Echenique, *Phys. Rev. Lett.* **86**, 488 (2001).
- ²⁶I. Yu. Sklyadneva, E. V. Chulkov, W.-D. Schöne, V. M. Silkin, R. Keyling, and P. M. Echenique, *Phys. Rev. B* **71**, 174302 (2005).
- ²⁷B. Hellsing, J. Carlsson, L. Walldén, and S.-Å. Lindgren, *Phys. Rev. B* **61**, 2343 (2000).
- ²⁸A. Eiguren, B. Hellsing, F. Reinert, G. Nicolay, E. V. Chulkov, V. M. Silkin, S. Hüfner, and P. M. Echenique, *Phys. Rev. Lett.* **88**, 066805 (2002).
- ²⁹B. A. McDougall, T. Balasubramanian, and E. Jensen, *Phys. Rev. B* **51**, 13891 (1995).
- ³⁰Ph. Hofmann, Y. Q. Cai, Ch. Grütter, and J. H. Bilgram, *Phys. Rev. Lett.* **81**, 1670 (1998).
- ³¹T. Balasubramanian, E. Jensen, X. L. Wu, and S. L. Hulbert, *Phys. Rev. B* **57**, R6866 (1998).
- ³²S.-J. Tang, Ismail, P. T. Sprunger, and E. W. Plummer, *Phys. Rev. B* **65**, 235428 (2002).
- ³³J. E. Gayone, S. V. Hoffmann, Z. Li, and Ph. Hofmann, *Phys. Rev. Lett.* **91**, 127601 (2003).
- ³⁴J. J. Paggel, D.-A. Luh, T. Miller, and T.-C. Chiang, *Phys. Rev. Lett.* **92**, 186803 (2004).
- ³⁵T. K. Kim, T. S. Sørensen, E. Wolfring, H. Li, E. V. Chulkov, and Ph. Hofmann, *Phys. Rev. B* **72**, 075422 (2005).
- ³⁶G. Grimvall, *The Electron-Phonon Interaction in Metals*, Selected Topics in Solid State Physics, edited by E. Wohlfarth (North-Holland, Amsterdam, 1981).
- ³⁷B. Hellsing, A. Eiguren, and E. V. Chulkov, *J. Phys.: Condens. Matter* **14**, 5959 (2002).
- ³⁸A. Eiguren, B. Hellsing, E. V. Chulkov, and P. M. Echenique, *Phys. Rev. B* **67**, 235423 (2003).
- ³⁹E. V. Chulkov, V. M. Silkin, and P. M. Echenique, *Surf. Sci.* **391**, L1217 (1997); **437**, 330 (1999).
- ⁴⁰J. E. Black and F. C. Shanes, *Surf. Sci.* **133**, 199 (1983).
- ⁴¹N. W. Ashcroft, *Phys. Lett.* **23**, 48 (1966).
- ⁴²I. Yu. Sklyadneva, A. Leonardo, P. M. Echenique, S. V. Eremeev, and E. V. Chulkov, *J. Phys.: Condens. Matter* **18**, 7923 (2006).
- ⁴³A. Eiguren, S. de Gironcoli, E. V. Chulkov, P. M. Echenique, and E. Tosatti, *Phys. Rev. Lett.* **91**, 166803 (2003).
- ⁴⁴M. Fuglsang Jensen, T. K. Kim, S. Bengio, I. Yu. Sklyadneva, A. Leonardo, S. V. Eremeev, E. V. Chulkov, and Ph. Hofmann, *Phys. Rev. B* **75**, 153404 (2007); I. Yu. Sklyadneva, A. Leonardo, P. M. Echenique, and E. V. Chulkov, *Surf. Sci.* (to be published).
- ⁴⁵U. O. Karlsson, G. V. Hansson, P. E. S. Persson, and S. A. Flodström, *Phys. Rev. B* **26**, 1852 (1982).
- ⁴⁶R. A. Bartynski, R. H. Gaylord, T. Gustafsson, and E. W. Plummer, *Phys. Rev. B* **33**, 3644 (1986).
- ⁴⁷F. Schiller, M. Heber, V. D. P. Servedio, and C. Laubschat, *Phys. Rev. B* **70**, 125106 (2004).
- ⁴⁸E. V. Chulkov, V. M. Silkin, and E. N. Shirykalov, *Surf. Sci.* **188**, 287 (1987); E. V. Chulkov and V. M. Silkin, *Solid State Commun.* **58**, 273 (1986).
- ⁴⁹P. B. Allen and M. L. Cohen, *Phys. Rev.* **187**, 525 (1969).
- ⁵⁰S. Baroni, S. de Gironcoli, A. Dal Corso, and P. Giannozzi, <http://www.pwscf.org>
- ⁵¹N. E. Zein, *Fiz. Tverd. Tela (Leningrad)* **26**, 3028 (1984) [*Sov. Phys. Solid State* **26**, 1825 (1984)].
- ⁵²S. Baroni, S. de Gironcoli, A. Dal Corso, and P. Giannozzi, *Rev. Mod. Phys.* **73**, 515 (2001).
- ⁵³M. Methfessel and A. T. Paxton, *Phys. Rev. B* **40**, 3616 (1989).
- ⁵⁴I. Campillo, V. M. Silkin, J. M. Pitarke, E. V. Chulkov, A. Rubio, and P. M. Echenique, *Phys. Rev. B* **61**, 13484 (2000).
- ⁵⁵L. J. Slutsky and C. W. Garland, *Phys. Rev.* **107**, 972 (1957).
- ⁵⁶I. Baraille, C. Pouchan, M. Causa, and F. Marinelli, *J. Phys.: Condens. Matter* **10**, 10969 (1998).
- ⁵⁷Ismail, Ph. Hofmann, E. W. Plummer, C. Bungaro, and W. Kress, *Phys. Rev. B* **62**, 17012 (2000).
- ⁵⁸R. Pynn and G. L. Squires, *Proc. R. Soc. London, Ser. A* **326**, 347 (1972).
- ⁵⁹D. M. Burnell and E. L. Wolf, *Phys. Lett.* **90A**, 471 (1982).
- ⁶⁰E. Bucher, V. Heine, K. Andres, J. P. Maita, and A. S. Cooper, *Phys. Rev. B* **6**, 103 (1972).
- ⁶¹A. C. Mota, P. Brewster, and R. Wang, *Phys. Lett.* **41A**, 99 (1972).
- ⁶²A. O. E. Animalu and V. Heine, *Philos. Mag.* **12**, 1249 (1965).
- ⁶³J. C. Kimball, R. W. Stark, and F. M. Mueller, *Phys. Rev.* **162**, 600 (1967).
- ⁶⁴C. Kittel, *Introduction to Solid State Physics* (Wiley, New York, 1976).
- ⁶⁵P. T. Sprunger, K. Pohl, H. L. Davis, and E. W. Plummer, *Surf. Sci.* **297**, L48 (1993).
- ⁶⁶A. F. Wright, P. J. Feibelman, and S. R. Atlas, *Surf. Sci.* **302**, 215 (1994).
- ⁶⁷V. M. Silkin and E. V. Chulkov, *Phys. Solid State* **42**, 1373 (2000) [*Fiz. Tverd. Tela (S.-Peterburg)* **42**, 1334 (2000)].
- ⁶⁸N. W. Ashcroft and N. D. Mermin, *Solid State Physics* (Saunders College Publishing, Fort Worth, TX, 1976).